Thermal engineering model of a heat exchanger with finned tubes made from porous carbon foam

Qijun Yu, Brian E. Thompson and Anthony G. Straatman

Department of Mechanical & Materials Engineering
University of Western Ontario, London, Ontario, Canada N6A 5B8

A thermal engineering model to represent heat transfer from porous carbon foam has been developed for use in design processes for heat exchangers with finned tubes. Characteristic parameters for carbon foam geometries, specifically exposed surface absolute roughness, exposed surface area factor, effective thermal conductivity, surface area to volume ratio and permeability, are calculated with a simple geometric model of a unit cube with spherical void surrounded by carbon-foam dendrites. The airside thermal resistance is calculated with an engineering model derived from conventional correlations that are extended to represent the effects of porosity. Specifically, airside convective heat transfer was modified, first, to account for the effects of roughness due to the porous surface and, second, to represent the recruitment of effective surface due to interstitial flow through the carbon matrix. The surface area recruitment was modeled as a function of the Reynolds and Darcy numbers, the friction factor, the contraction and the expansion loss coefficient of the fin channel. Using this model, an optimum permeability can be predicted because the exposed surface factor and the effective thermal conductivity decrease as porosity increases. Comparisons with measured results suggest that the present thermal-engineering model calculates heating conservatively, specifically about 11% less than the measured heat load.

1. INTRODUCTION

Porous carbon foam developed at the Oak Ridge National Laboratory (ORNL) exhibits high thermal conductivity [1]. Figure 1 shows carbon foam has open surfaces with ragged dendrites, and this suggests convective heat transfer will differ from that on smooth walls [2]. Measured cooling rates from a prototype air-water radiator made of carbon foam [3] confirm that carbon foam has the potential to increase the airside heat transfer coefficient due to its unique physical and geometric characteristics.

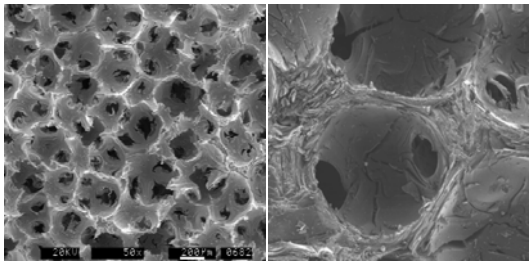

(a) (b)

Figure 1: *(a) Electron micrograph of the Carbon Foam surface; (b) Electron micrograph of the Carbon Foam, the porosity=0.9 and the pore diameter=400 um.*

Understanding the heat-transfer mechanisms and representing their effects in thermal-design models are the subjects of the present research program. This paper presents a thermal engineering model that was developed for the design of air-to-water heat exchangers with fins made of carbon foam. Emphasis is placed the calculation of thermal resistance and pressure loss due to carbon-foam fins.

2. UNIT CUBE GEOMETRIC MODEL

In order to obtain the values of the geometry parameters for 1) exposed surface absolute roughness, 2) exposed surface area factor, 3) effective thermal conductivity, 4) surface area to volume ratio and 5) permeability of the porous carbon foam, a geometric model must be established. The surface areas of the fin channel and the pore block, and the heat transfer coefficient of the solid-to-air interface at the fin channel and the pore block are necessary for determining the overall heat transfer coefficient on the air side (carbon foam fin side). These are determined using the geometry parameters of the foam, the fin configurations, and well-

established thermal correlations. A unit cube geometry model is created for the Carbon Foam and assumptions for the unit cube geometry model are set up according to the geometric characteristics described in the Patent file [4] by the Carbon Foam inventors as follows:

1. Each cell has a spherical void at the center of each unit cube;

2. Cells are close packed and regularly arranged so that each pore connects with 6 adjacent pores;

3. The pore structure can be divided into three types:

a. An isolated pore structure exists when the porosity is smaller than $\pi/6$ (≈ 0.525);

b. An untouched solid pore exists when the porosity is greater than 0.30719π (≈ 0.965)

c. An interconnected pore structure exists when the porosity is between $\pi/6$ and 0.30719π.

This geometry model developed herein is only valid for the inter-connected pore structure, which has porosity between $\pi/6$ and 0.30719π.

Averaging, normalizing and equivalent methods were used to determine the geometric parameters. Figure 2 (a) shows a block consisting of number of pores and (b) shows the details of the single unit cube geometry model.

1. H = Cube height
2. D = Pore diameter (average)
3. R=Pore radius (R=D/2)
4. d= the inter-connected pore channel diameter,

$$d = 2\sqrt{R^2 - \left(\frac{H}{2}\right)^2} \qquad (1)$$

5. h = spherical cap height of the pore,

$$h = R - \frac{H}{2} \qquad (2)$$

6. c = strut width at the center plane of the solid,

$$c = \frac{H - d}{2} \qquad (3)$$

By the definition of porosity ---void divided by the sum of the void and the solid --- the porosity ε of the pore structure is given as:

$$\varepsilon = \frac{\left(\frac{4}{3}\pi R^3 - 6\frac{1}{3}\pi h^2(3R - h)\right)}{H^3} \qquad (4)$$

The value of the height of the unit cube is determined by solving the following cubic equation for given pore radius (R) and porosity (ε):

$$\left(3\varepsilon + \frac{3}{4}\pi\right)H^3 - 9\pi R^2 H + 8\pi R^3 = 0 \quad (5)$$

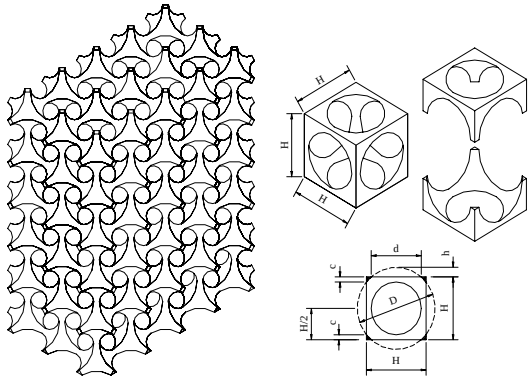

(a) (b)

Figure 2: *(a) A block consisting of a number of pores and (b) Details of the single unit cube geometry model.*

3. PORE STRUCTURE PARAMETERS

Geometric parameters of the carbon foam are determined using the given values of the pore diameter, porosity and the unit cubic height (H) obtained from equation (5). The desired parameters are: the absolute surface roughness, the opened pore surface area factor, the pore hydraulic diameter, the surface area to volume ratio, the permeability and the effective thermal conductivity. Expressions for each are now given in turn.

3.1 Absolute Surface Roughness

The absolute surface roughness factor, RA, is a function of d, R and H and is described by:

$$RA = \frac{d}{2} = \sqrt{R^2 - \left(\frac{H}{2}\right)^2} \qquad (6)$$

3.2 Opened Pore Surface Area Factor

The opened pore surface area includes two parts: 1) the flat cross-section surface area; 2) the void phase spherical wall surface area.

1) The flat cross-section surface area is computed from two portions: (i) from 0 to c and (ii) from c to H/2 as shown in Figure 3:

(i) from 0 to c:

$$S_{avg\ 1} = \frac{1}{c}\int_0^c S1\,dy \qquad (7)$$

where: $S1 = H^2 - \pi\left(R^2 - (R-h-y)^2\right)$

(ii) from c to H/2:

$$S_{avg\ 2} = \frac{1}{\left(\frac{H}{2} - c\right)}\int_c^{H/2} S2\,dy \qquad (8)$$

where: $S2 = H^2 - \pi r^2 + 2r^2(\theta - Sin\theta)$,

$$\theta = 2Cos\left(\frac{H}{2r}\right)$$

and: $r = \sqrt{R^2 - (R-h-y)^2}$

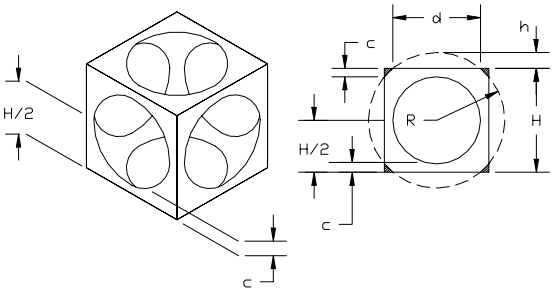

Figure 3: *Single unit cube.*

The average flat cross-section area, S_{favg}, is then obtained from:

$$S_{favg} = \frac{2\left(S_{avg\,1}c + S_{avg\,2}\left(\frac{H}{2} - c\right)\right)}{H}$$

(9)2) The void phase spherical wall surface area, S_s (assuming the pore is cut at the pore center), is given as:

$$S_s = 2\pi R(R - 3h) \qquad (10)$$

The total averaged opened surface area at the exposed layer, S_{tavg}, is given as:

$$S_{tavg} = S_{favg} + S_s \qquad (11)$$

Finally, the opened pore surface area factor, SF, is given as:

$$SF = \frac{S_{tavg}}{H^2} \qquad (12)$$

The exposed surface area factor decreases as the porosity increases, reaches a maximum value of 2.12 at a porosity of $\pi/6$, and reaches 1 at a porosity of $\pi 639/23$ for pore diameters between 60 and 600 um.

3.3 Hydraulic diameter of the pore

The hydraulic diameter of the pre is given as:

$$dh_{pore} = \frac{4Void\ \_Volume}{Void\ \_Surface\ \_Area}$$

$$= \frac{\varepsilon H^3}{2S_s} \qquad (13)$$

$$Void\ \_Volume = \varepsilon H^3 \qquad (14)$$

$$Void\ \_Surface\ \_Area = 2S_s \qquad (15)$$

3.4 Surface Area to Volume Ratio

The pore's spherical wall surface area per 1 cubic meter of the carbon foam is given

$$\beta = \frac{2S_s}{H^3} \qquad (16)$$

3.5 Permeability

3.5.1 Permeability of un-deflected pore structure

For a quarter-spherical-particle (solid phase) pore structure on a simple cube, shown in Figure 4 (a), the permeability is determined from the following equation proposed by Nakayama [5]:

$$K = \frac{\varepsilon^3 DE^2}{147(1-\varepsilon)^2} \qquad (17)$$

where DE is the equivalent solid particle diameter.

To compute the permeability of the carbon foam pore structure shown in Figure 4 (b) using the above equation, an equivalent quarter -spherical-particle pore structure with the same solid volume as the inter-connected pore structure is first introduced to represent the carbon foam pore structure. The equivalent particle diameter of the carbon foam, DE=2RE as shown in Figure 4 (a), is determined by:

$$\frac{\pi}{6}DE^3 = (1-\varepsilon)H^3 \qquad (18)$$

Second, the same equivalent quarter spherical particle pore structure with the same solid wall surface area as the inter-connected pore structure is introduced to represent the carbon foam pore structure such that

$$\pi DE^2 = \beta H^3 \qquad (19)$$

The quarter spherical particles pore structure must satisfy both volume and surface equivalent that gives

$$DE = \frac{6(1-\varepsilon)}{\beta} \qquad (20)$$

this equation is the same as proposed by Dullien [6] for sphere particle bed pore structure.

Substituting (19) into equation (16), the permeability of the inter-connected pore structure of the carbon foam is determined by

$$K = \frac{36\varepsilon^3}{147\beta^2} \qquad (21)$$

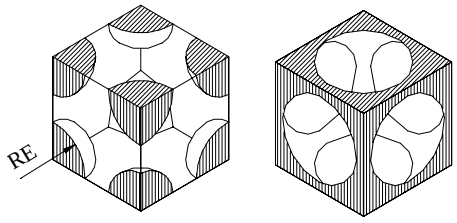

(a) (b)

Figure 4: *Equivalent spherical particle cube.*

3.5.2 Permeability of deflected pore structure

Figure 5 (a) and (b) show the unreal and real pore structure when the porosity is greater than the critical porosity ε' at which the permeability reaches it's peak value K'. In order to hold and maintain the inter-connected pore structure the strut neck at the center plan of the unit cube must be big enough to support the pore structure, and it cannot reach zero even when the porosity reaches 96.5%. The wall material flows to the center plane of the unit cube to keep the strut width c greater than a certain value so that it can hold the pore structure as shown in Figure 5 (c).

The critical porosity ε' or the peak value of the permeability K' of the carbon foam can only be determined by experiments.

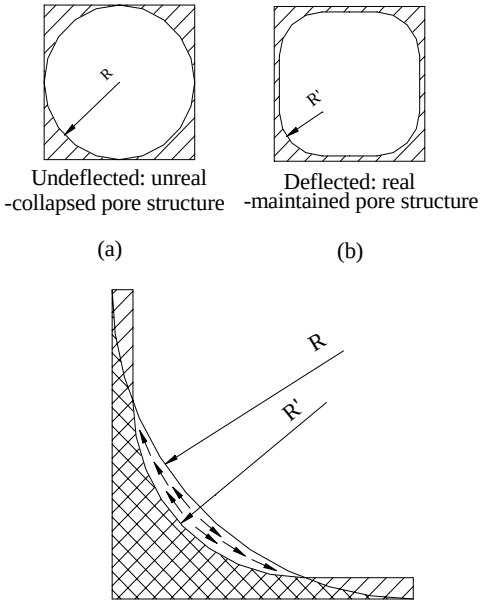

Figure 5: *Material flow of deflected pore.*

The permeability for porosities greater than the critical porosity can be determined using linear interpolation, i.e.,

$$K_{(\varepsilon>\varepsilon')} = K_{(\varepsilon')} - \frac{\left(K'_{(\varepsilon')} - K_{(2\varepsilon'-0.965)}\right)}{\left(0.965-\varepsilon'\right)}\left(\varepsilon-\varepsilon'\right) \qquad (22)$$

3.6 Effective Thermal Conductivity

To obtain the effective thermal conductivity of carbon foam the same method for determining permeability is going to be employed again. However this time an equivalent unit cubic of square bars with same porosity is introduced

instead of combining the same volume and surface area. The heat flux is in the direction of the fin height that is the direction of the temperature gradient. No convection and radiation in the pores and local thermal equilibrium are assumed. Figure 6 shows the detail of the equivalent process.

The square bar height a is determined by solving the cubic equation (23) derived from the equivalent process.

$$a^3 - \frac{3}{4}a^2 + \frac{(1-\varepsilon)}{16}H^3 = 0 \qquad (23)$$

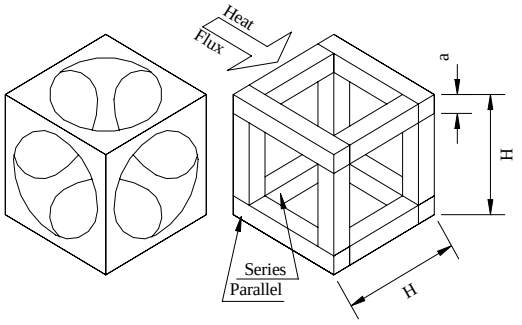

Figure 6: *Equivalent square bar structure*

Figure 7 shows the details of simplifying the processes of the pore structure. Using an electrical analogy for the heat this problem can be represented as shown in Figure 7 (d) and described schematically as shown in Figure 8.

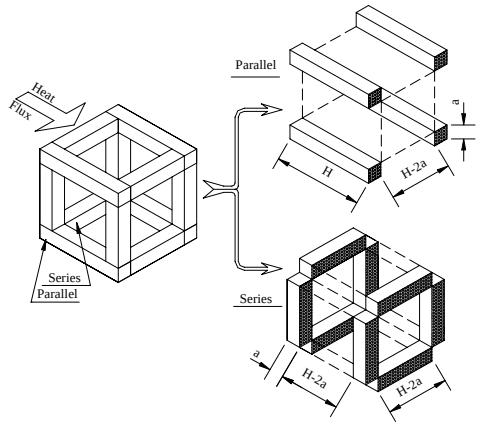

(a) (b)

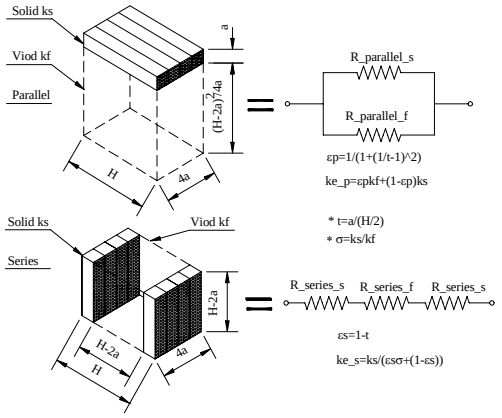

(c) (d)

Figure 7: *The detail processes for determining the effective thermal conductivity*

The effective thermal conductivities for the parallel and series portions shown in Figure 8 (b) can be computed from equations reported by Hadley [7].

1) For the parallel portion

$$ke_p = \varepsilon_p k_f + (1-\varepsilon_p)k_s \qquad (24)$$

2) For the series portion

$$ke_s = \frac{k_s}{\varepsilon_s \sigma + (1-\varepsilon_s)} \qquad (25)$$

ke_p is the effective thermal conductivity for the parallel bars and ke_s for the series bars shown in Figure 8 (b). k_f is the thermal conductivity of air and k_s is the thermal conductivity of the solid. σ is the ratio of k_s/k_f. ε_p is calculated to be:

$$\varepsilon_p = \left(1 + \left(\frac{1}{t} - 1\right)^2\right)^{-1} \qquad (26)$$

where t is the normalized thickness of the bar,

$$t = 2a/H \qquad (27)$$

and ε_s is calculated to be

$$\varepsilon_s = 1 - t \qquad (26)$$

The effective thermal conductivity of the system is then determined by

$$ke = \varepsilon ke_p + (1 - \varepsilon_P)ke_s \qquad (27)$$

where,

$$\varepsilon = 1 - 2t + 2t^2 \qquad (28)$$

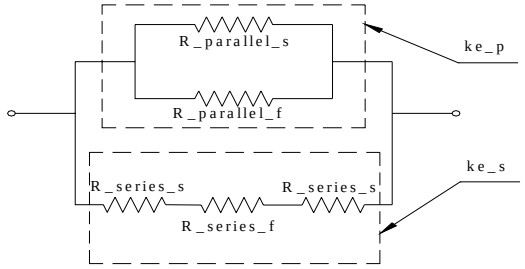

Figure 8: *Equivalent heat flow resistance circuit.*

4. THERMAL ENGINEERING MODEL

The air-flow behavior in the fin channel plays a vital role in determining the heat transfer coefficient and friction loss. The open pore structure on the Carbon Foam fin surface performs as a turbulence promoter because of the sharp edges on the fin surface, and as sublayer interrupter because of its openinter-connected pore structure.

The effects of the pore structure on the flow behavior in the fin channel are determined by the pore diameter and porosity, fin thickness, fin height, fin spacing, and fin tip clearance.

The Darcy equations and continuity equations, together with the state equations are employed to compute the air velocities in the fin channel and in the inter-connected pore channel.

4.1 Fin and Tube Configurations

Figure 9 shows the details of the fin and tube configuration. In figure 9, the parameters are given as:

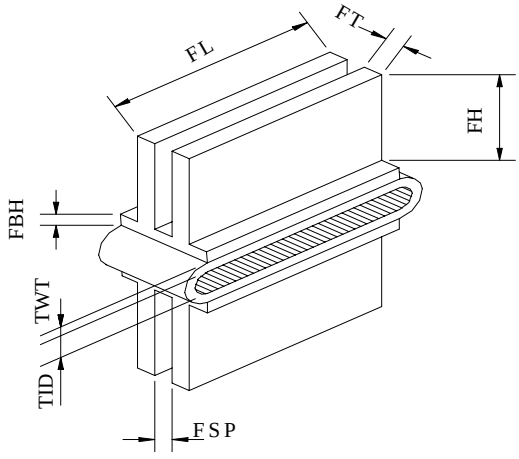

Figure 9: *Fin and tube configurations*

FT = fin thickness

FH = fin height (along the growing direction of the carbon foam)

FL = fin length (along the air flow direction)

FSP = fin space, determined by

FBH = fin base height

TWT = liner tube wall thickness

TID = liner tube inside diameter

4.2 Air Velocities and Pressure Drops

Figure 10 shows the geometrical configurations and the approximate air velocity profiles in the fin channel and the pore block [8].

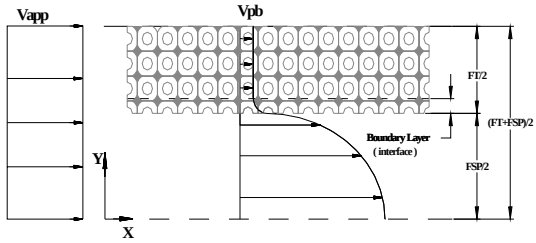

Figure 10: *Air velocity profile in fin channel*

4.2.1 *Pressure drop in the fin channel*

In the fin channel the friction and dynamic pressure loss is computed by the Darcy-Weibach equation [9]:

$$\Delta P_{fin} = \left(f' \frac{FL}{Dh_{fc}} + C \right) \rho_{avg} V_{fcavg}^{\ 2} \qquad (29)$$

where V_{fcavg} is the air mean velocity at the air average temperature in the fin channel, determined later by solving the continuity and Darcy equations. ρ_{avg} is the air density at the air average temperature.

f' is the friction factor in the fin channel without taking account of the air flow through the pore block, and is also given from [9]:

$$f' = 0.11\left(\frac{RA}{Dh_{fc}} + \frac{68}{\mathrm{Re}'_{fc}}\right)^{0.25} \quad (30)$$

where Re'_{fc} is the Reynolds number in the fin channel without taking account of the air flow through the pore block, determined by

$$Re'_{fc} = \frac{V'_{fcavg} Dh_{fc}}{\nu_{avg}} \quad (31)$$

where V'_{fcavg} is the air velocity at the air average temperature in the fin channel without taking account of the air flow through the pore block. Since its effect on the friction factor is negligible, it can be computed by:

$$V'_{fcavg} = \frac{S_{front}}{S_{free}} \frac{\rho_o}{\rho_{avg}} V_{app} \quad (32)$$

where S_{front} is the frontal flow area before the fin channel, and S_{free} is the free flow area in the fin channel; ρ_o is the air density at the air inlet temperature. V_{app} is the air approach velocity at the air inlet conditions (inlet temperature and pressure).

Dh_{fc} is the hydraulic diameter of the fin channel defined as:

$$Dh_{fc} = \frac{4Surface\_Area_{fin\_channel}}{Pameter_{fin\_channel}} \quad (33)$$

The sudden contraction pressure loss coefficient at the fin channel entrance, Cc, and the sudden expansion pressure loss coefficient at the fin channel exit, Ce are given as [10]:

$$Cc = 0.42\left(1 - \left(\frac{Dh_{fc}}{Dh_{front}}\right)^2\right) \quad (34)$$

$$Ce = \left(1 - \left(\frac{Dh_{fc}}{Dh_{back}}\right)^2\right)^2 \quad (35)$$

D_{hfront} and D_{hback} are the equivalent hydraulic diameters of the free flow area before the entrance and after the exit of the fin channel, and $Dh_{front} = Dh_{back}$.

4.2.2 *Pressure drop in the Inter-connected pore channel*

In the pore block the pressure loss, neglecting the inertial term, can be determined by the Darcy equation from [11] :

$$\Delta P_{pb} = \frac{\mu_{film}}{K} V_{pbfilm}\, FL \quad (36)$$

4.2.3 *Calculation of the air velocities*

V_{fcavg} is the air velocity at the air average temperature in the fin channel, and can be determined by solving a set of continuity and Darcy equations:

$$S_{front} V_{app} \rho_o = S_{fc} V_{fc} \rho_o + S_{pb} V_{pb} \rho_o \quad (37)$$

$$\left(f' \frac{FL}{Dh_{fc}} + C\right) \frac{\rho_{avg} V_{fcavg}^2}{2} = \frac{\mu_{film}}{K} V_{pbfilm}\, FL \quad (38)$$

$$V_{fcavg} = \frac{\rho_o}{\rho_{avg}} V_{fc} \quad (39)$$

where:

$$V_{pbfilm} = \frac{\rho_o}{\rho_{film}} V_{pb} \quad (40)$$

Solving equations (37) to (40) yields

$$S_{front} V_{app} \rho_o = S_{fc} \rho_{avg} V_{fcavg} + S_{pb} \rho_{film} A V_{fcavg}^2 \quad (41)$$

$$A = \frac{1}{2}\left(f' \frac{FL}{Dh_{fc}} + C\right) \frac{\rho_{avg} K}{\upsilon_{film} FL} \quad (42)$$

By solving the above equation (42), V_{fcavg} can be determined and then $V_{pbfilm,}$ which are the air velocities in the fin channel at the air average temperature and the inter-connected pore channel at the film temperature respectively.

4.3 Surface Area Recruit Coefficient

The air pressure drops across the fin channel and the pore block always automatically balance with each other in any thermal conditions as shown in equation (38). The surface area recruitment coefficient in the inter-connected pore channel, RC, is defined as the ratio of the air velocity in the pore block at the film temperature and the air

mean velocity in the fin channel at the air average temperature

$$RC = \frac{V_{pbfilm}}{V_{fcavg}} \tag{43}$$

The value of the RC can be calculated by using the obtained values from equation (41). However the RC can be represented by dimensionless factors such as Reynolds number and Darcy number. The following shows deriving the RC. Equation (38) can be rearranged as

$$\frac{V_{pbfilm}}{V_{fvavg}} = f\frac{\rho_{avg}V_{fcavg}}{2Dh_{fc}}\frac{K}{\mu_{film}} + C\frac{\rho_{avg}V_{fcavg}}{2\mu_{film}FL}K$$

$$= \frac{f}{2}\frac{\rho_{avg}V_{fcsvg}Dh_{fc}}{\mu_{avg}}\frac{K}{H'^2}\frac{\mu_{avg}}{\mu_{film}}\left(\frac{H'}{Dh_{fc}}\right)^2 + \frac{C}{2}\frac{\rho_{avg}V_{fcsvg}Dh_{fc}}{\mu_{avg}}\frac{K}{H'^2}\frac{\mu_{avg}}{\mu_{film}}\frac{H'^2}{Dh_{fc}FL}$$

$$= \frac{f}{2}\delta^2 \,\mathrm{Re}Da\mu' + \frac{C}{2}\delta^2 \,\mathrm{Re}Da\mu'$$

then we get

$$RC = \left(\frac{f\delta^2 + C\delta'^2}{2}\right)\mathrm{Re}\,Da\mu' \tag{44}$$

Re is the Reynolds number of the air flow in the fin channel at the air average temperature, and is given as:

$$\mathrm{Re} = \frac{V_{fcavg}\,Dh_{fc}}{\upsilon_{avg}} \tag{45}$$

f is the friction factor, but here f is calculated from the air mean velocity at the air average temperature in the fin channel with taking account of the air flow through the pore block, and is given

$$f = 0.11\left(\frac{RA}{Dh_{fc}} + \frac{68}{\mathrm{Re}}\right)^{0.25} \tag{46}$$

Da is the Darcy number, and is given

$$Da = \frac{K}{H'^2} \tag{47}$$

where H' is the length scale of the flow cross-section (including the fin channel and the pore block), and is given as:

$$H' = \sqrt{\left(FH + \frac{FTP}{2}\right)\left(\frac{FT + FSP}{2}\right)} \tag{48}$$

δ is the normalized length scale of the flow cross-section, and δ' is the apparent normalized length scale of the flow cut-section along the air flow direction (or say along the air flow direction), and is given as:

$$\delta = \frac{H'}{Dh_{fc}} \tag{49}$$

$$\delta' = \frac{H'}{\sqrt{Dh_{fc}\,FL}} \tag{50}$$

C is dynamic pressure loss coefficient (the sum of the entrance and the exit, C=Ce+Cc). μ' is the air viscosity ratio between the average temperature and the film temperature

$$\mu' = \frac{\mu_{avg}}{\mu_{film}} \tag{51}$$

4.4 Heat Transfer Model

Figure 11 shows the thermal resistance elements of the carbon foam finned tube. The Total resistance is computed by

$$R_{total} = R_1 + R_2 + \left(\frac{1}{R_7} + \left(R_3 + R_4 + \left(\frac{1}{R_5} + \frac{1}{R_6}\right)^{-1}\right)^{-1}\right)^{-1} \tag{52}$$

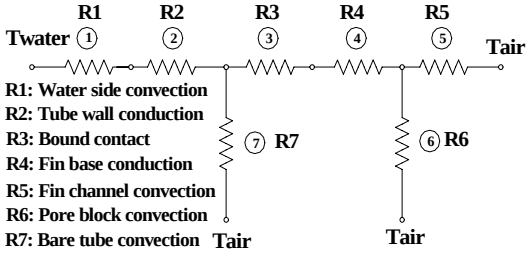

Figure 11: *Heat transfer model.*

The surface area recruitment coefficient is used to account for the heat transferred in the pore channel by adding the surface area recruited in

the pore channel to the open pore surface area in the fin channel such that

$$R_{airconv} = \left(\frac{1}{R_5} + \frac{1}{R_6} \right)^{-1} \quad (53)$$

4.4.1 *Total heat transfer surface area at air side*

The air-side total heat transfer surface area is computed to be

$$S_{tair} = N_{fin} S_{solid\_fin} SF_t \quad (54)$$

where N_{fin} is the total fin number, and $S_{solid\text{-}fin}$ is the effective surface area of the solid fin. SF_t is the total surface area factor and is given

$$SF_t = SF + \frac{\beta \Lambda RC}{S_{solid\_fin}} \quad (55)$$

where Λ is the volume of the carbon foam fin.

4.4.2 *Thermal resistances at the air-side*

The thermal resistance in the fin channel accounting the effects of the heat transferred in the inter-connected pore channel is given as:

$$R_{airconv} = \frac{Dh_{fc}}{k_{favg} S_{tair} \eta_o Nu} \quad (56)$$

where k_{favg} is the air thermal conductivity at the air average temperature. The Nusselt number in the fin channel is determined by well-established correlations depending on the Reynolds number. Finally, η_o is the fin overall surface efficiency.

FHe is the effective height of the carbon foam fin and ke is the effective thermal conductivity of the carbon foam fin at the film temperature.

Correlations of Nusselt numbers and friction factors for the inter-connected pore channel, fin channel and water tube are employed from [9, 10, 11, 12, 13, 14, 15, 16, 17, 18, 19].

4.5 Core Design

The Effectiveness-NTU methods are employed to size the core of the heat exchanger [20]

$$Ntu = \frac{S_{tair} U}{C_{min}} = \frac{1}{R_{total} C_{min}} \quad (57)$$

where U is the overall conductance for heat transfer based on the air side total heat transfer surface area including both the open and inter-connected surfaces. C_{min} is the smaller of the hot and cold fluid capacity rates.

5. VALIDATION

Table 1 is a summary of specification of two carbon foams made by ORNL and the effective thermal conductivity values obtained from this model. The maximum errors are less than 2% for Foam A and less than 6.5% for Foam B.

Table 1: *Summary of foam specification including estimate from present model*

Item	D um	ε %	*ks W/mK*	*ke W/mK*	
				Measured *	Present Model
Foam A	60	73	1200	127	125
Foam B	350	75	1700	175	164

* Measured data are posted on ORNL website: www.ms.ornl.gov/cimtech/cimtech.html

Table 2 presents a brief comparison of the performance data obtained from testing and calculation for an air radiator made of carbon foam finned tubes by ORNL[3], at the same thermal conditions: water flow of 0.29 kg/s at 98.8 ºC inlet temperature; air flow rate of 0.69 kg/s at 31.6 ºC inlet temperature.

Table 2: *Summary of measured and predicted water temperatures from test heat exchanger*

	Measured	Present Model	E %
Water out T ºC	86	88	2.3
Heat Load kW	14.82	13.16	11.2

For the radiator considered at the above thermal conditions the present model yields a performance rating of 0.888. This means that the model gives a conservative factor of 11.2% in terms of heat load, see Table 2, which is desirable, acceptable and safe for engineering practicing.

6. PERFORMANCE IMPROVEMENT

The air radiator as mentioned above was redesigned using optimized pore structure and fin configurations by Orthogonal Design method [21]. Figure 12 shows the improvement potential

of the new air radiator designed by the presenting thermal engineering model.

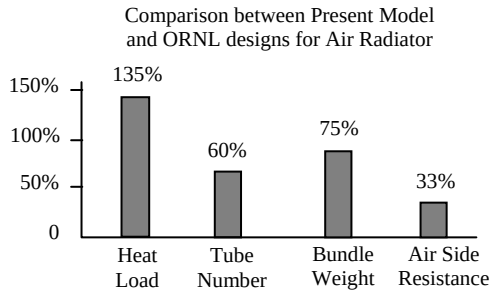

Figure 12: *Improvement of the new design.*

7. CONCLUDING REMARKS

A thermal engineering model for the design of air to water heat exchangers made with carbon foam finned tubes has been developed based on a unit cube geometry model and well-established correlations for channel flow. Surface area recruitment is modeled as a function of the Reynolds and Darcy numbers, the friction factor, the contraction and the expansion loss coefficient of the fin channel.

Results show that the exposed surface area factor decreases as the porosity increases. Permeability reaches a peek value at a certain porosity. Effective thermal conductivity is a function of the thermal conductivity of the solid carbon and the porosity of the carbon foam. Comparisons with measured effective thermal conductivity are within 6.5% and calculated heat load is about 89% of measured values, both of which are adequate for heat-exchanger design purposes.

8. ACKNOWLEDGEMENT

This work is sponsored by Canada's Department of Natural Resources in collaboration with Oak Ridge National Laboratory.

9. BIBLIOGRAPHY

[1] Jore Sanchez-Cornado, D.D.L. Chung, " Thermomechanical behavour of a graphite foam," Carbon Vol. 41, pp. 1175-1180, 2003.

[2] Klett, J. W., Hardy, R., Romine, E., Walls,C,. Burchell, T., " High thermal-conductivity, mesophase-pitch-derived carbon foam: effect of precursor on structure and properties, " Carbon, Vol. 38: pp 953-973, 2000.

[3] R.D. Ott, A. Zaltash, J.W. Klett, " Utilization of a graphite foam radiator on a natural gas engine-driven heat pump, " Proceedings of IMECE'02, ASME, 2002.

[4] James W. Klett, " Process for making carbon foam", United State Patent, Patent number: 6,033,506, 2000.

[5] A. Nakayama and F. Kuwahara, " Numerical modeling of convective heat transfer in porous media using microscopic structures," in Kambiz Vafai, Hamid A. Hadim, eds. Handbook of Porous Media, pp.449, Marcel Dekker, 2000.

[6] Dullien FAL, " Porous media fluid transfer and pore structure." New York: Academic Press, 1979.

[7] G.R. Hadley, " Thermal Conductivity of packed metal powders," Int. J. Heat Mass Transfer. Vol. 29, No.6, pp. 909-920, 1986.

[8] A.V.Kuznetsov, "Analytical studies of forced convection in partly porous configurations," In: Kambiz Vafai, Hamid A. Hadim, eds. Handbook of Porous Media, pp 272-273, Marcle Dekker, Inc., New York, 2000.

[9] R.J. Tsal, H.F. Behls, R. Mangel, " T-method duct design, part III: simulation," ASHRAE Transactions, 96(2), 1990.

[10] Frank M. White, " Fluid Mechanics ", 5th Edition, pp 389-390, McGraw-Hill, New York, 2000.

[11] Adrain Bejan, " Porous Media, " In: Ardian Bejan, Allan D. Kraus, eds. Heat Transfer Handbook, pp. 1135, 2003.

[12] P.Teertstra, M.M. Yovanovich and J.R.Culham, " Analytical forced convection modeling of plate fin heat sinks", Journal of Electronics Manufacturing, Vol.10, No.4 253-261, 2000.

[13] Kar K, Dybbs A. " Internal heat transfer coefficients of porous media", In: Beck JV, Yao LS, eds. Heat Transfer in Porous Media HTD-22, ASME, 1982.

[14] Gamson BW, Thodos G, Hougen OA. " Heat, mass and momentum transfer in the flow gases though granular solid". Transactions of AIChE 39:1-35,1943.

[15] R.H.S. Winterton, " Technical Notes: Where did the Dittus and Boelter equation come from? " Int. J. Heat Transfer. Vol. 41 Nos 4-5, pp. 809-810, 1998.

[16] V. Genielinski, " New equation for heat and mass transfer in turbulent pipe and channel flow " Int. Chem. Eng., Vol. 16, No.2, pp. 359-367, April 1976.

[17] S.W. Churchill, M. Bernstein, " A correlating equation for forced convection from gases and liquids to a circular cylinde in crossflow ", Transactions of the ASME, Vol. 99, pp. 300-306, May 1977.

[18] Petukhov, B.S., in T.F. Irvine and J.P. Hartnett., Eds., Advances in Heat Transfer, Vol. 6, Academic Press, New York, 1970.

[19] Sieder, E. N., and G.E. Tate, " Heat transfer and pressure drop of liquid in tubes ", Ind. Eng. Vol. 28, No.12, pp. 1429-1435, 1936.

[20] W. M. Kays, A. L. London, " Compact Heat Exchangers", three Edition, pp 14–24, McGraw-Hill Book Company, New York, 1985.

[21] Hedayat, A.S., Sloane,N.J.A., Stufken, J., Orthogonal Arrays-Theory and Applications, pp. 122, Springer-Verelag, New York, 1999.